# Experimental Verification of Actual Behaviour, Failure Mechanism and Load-Carrying Capacity of Floor and Roof Thin-Walled Ferro-Cement Panels

Marcela Karmazínová and Jindrich Melcher

***Abstract*—**The paper is focused on problems of the experimental verification of the actual behaviour, failure mechanism and mainly load-carrying capacity of thin-walled ferro-cement panels, which are developed for the usage in floor or roof slab horizontal structures. In the paper the overview and description of the realization and results of the loading tests of three types of ferro-cement panels with accent to the evaluation of their load-carrying capacity and its comparison with the theoretical analysis results. The main aim of the loading tests was to verify and evaluate the configuration of the panels, especially the arrangement and dimensions of the reinforcement from the viewpoint of its suitability and efficiency and in common with respect to the reaching reliable structural design. For the realization of the experimental verification the vacuum loading test method as one of the most effective loading procedures has been applied.

***Keywords*—**Ferro-cement, thin-walled panel, floor, roof, slab, experimental verification, actual behaviour, failure mechanism, load-carrying capacity, resistance, loading test, theoretical analysis.

## I. Introduction

THE structural ferro-cement components are composed of materials based on cement mortar and extremely slender steel reinforcement. The resulting products made of this material are characterized by the total slab thickness in the range from 20 to 50 mm. The base is usually small-grained cement mortar; physical-mechanical properties are provided by steel mesh, as a rule.

This material solution is relatively technically simple and can decrease material and overall costs, in general, compared to classic reinforced concrete. The economically positive characteristics have been recently taken as a reason for the wide expansion of ferro-cement structural elements to the underdeveloped world. These components can be used both in the housing buildings and in the agriculture and industry. The common attribute of this solution is material saving contrary to the comparable solution based on classic reinforce concrete, where it is necessary to take into account the structural durability, which is provided just by enough reinforcement protection increasing the overall dimension of the panel.

The characteristic tensile-bending strengths of ferro-cement matrix are higher than strengths of normal concrete. Also the high toughness under mechanical impact load is the important mechanical characteristics. However, the actual behaviour of the panel significantly depends on its particular shape, production technology and properties of matrix.

Manuscript received January 4, 2013. This work was supported in part by the Czech Ministry of Education, Youth and Sports under the project of the research centre CZ.1.05/2.1.00/03.0097 "AdMaS" and the project of the university specific research FAST S-11-32/1252.

Marcela Karmazínová, Faculty of Civil Engineering at the Brno University of Technology, Brno, Czech Republic (corresponding author to provide phone: +420 541 147 310; fax: +420 549 245 212; e-mail: karmazinova.m@fce.vutbr.fce.vutbr.cz).

## II. Description of Test Specimens

For the floor and roof component, the simple shape of the prefabricated component has been chosen and subsequently verified by loading tests.

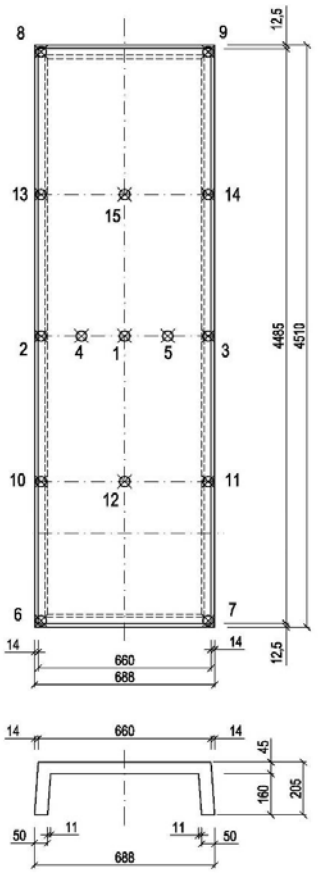


Fig. 1 Scheme of ferro-cement panel for floor or roof structure

The arrangement of test specimens is based on the structural detailing of newly developed ferro-cement panels for the slab horizontal floor structure. The nominal plan dimensions of this panel are 4 500 x 690 mm. The actual (measured) dimensions of the test specimens are seen in the scheme in Fig. 1. The rectangular floor component is stiffened by ribs of the total height of 205 mm, which are located on the edges of the 45 mm thick slab.

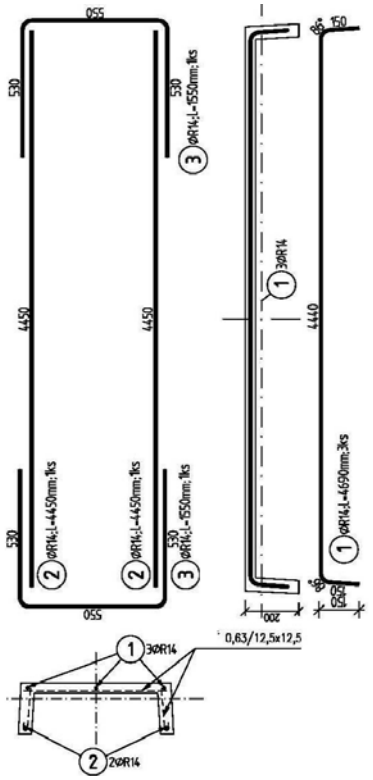


Fig. 2 Main reinforcement of ferro-cement panel (taken from [2])

It was assumed to test 3 specimens in total – test specimens *"A"* ( ≡ 1), *"B"* ( ≡ 2) and *"C"* ( ≡ 3) – aimed to verify the influence of different types of reinforcement on the actual behaviour of panels. However, during the production and transport process the failure of *"B"* specimen occurred, thus one another new specimen *"D"* with the same configuration as the origin specimen *"B"* ( ≡ 2) has been produced.

The main longitudinal reinforcement of the test specimens is represented by 5 reinforcing bars, that means 1 bar on the bottom edge of each longitudinal ribs and another 3 bars reinforcing the slab, which are placed on the top longitudinal edges and in the middle of the slab panel. The configuration and location of the reinforcement of test specimens is drawn in the scheme in Fig. 2 (main bars only, excluding reinforcing mesh). The overview of test specimens including their self weights and basic description of their reinforcement is shown in Table 1.

More data oriented to the detailed reinforcement of the test specimens, especially with regards to the arrangement of the transverse and structural reinforcement and also reinforcing wire mesh have been included in the technical production documentation of the contracting authority, which has ordered the realization of loading tests.

Table 1 Overview of test specimens

| **Specimen**<br>**Self weight [kg]** | **Informative description of the reinforcement** |
|---|---|
| ***"A"*** ( ≡ 1)<br>485 | Ø R14 – bottom edge of longitudinal ribs;<br>Ø R8 – longitudinal edge and middle of slab; reinforcing wire mesh in slab |
| *"B"* ( ≡ 2) | Failed during production → not tested |
| ***"C"*** ( ≡ 3)<br>479 | Ø R14 – bottom edge of longitudinal ribs;<br>Ø R14 – longitudinal edge and middle of slab; no reinforcing wire mesh |
| ***"D"*** ( ≡ 2)<br>456 | Ø R8 – bottom edge of longitudinal ribs;<br>Ø R8 – longitudinal edge and middle of slab; no reinforcing wire mesh |

During the production of test specimens material properties have been investigated [2]. The mechanical parameters of ferro-cement matrix have been measured using material testing. To obtain the strengths in compression, the material tests on the cubes subjected to compression were applied. The corresponding cylindrical strengths $f_c$ have been determined using the usual relation in the form of $f_c = 0.8\, f_{cc}$. To obtain the tensile and tensile-in-bending properties, the material tests on the prisms subjected to tension and bending were used. The mechanical parameters of reinforcement steel have not been measured, the values of required properties have been taken according to European Standard EN 1992 [31] for adequate used reinforcement. The basic mechanical properties of both materials are listed in Table 2 (all values taken from [2]).

Table 2 Material properties of ferro-cement panels (taken from [2])

| **Ferro-cement matrix** – properties measured | | |
|---|---|---|
| Tensile-bending strength $f_{ctfl,m}$ (mean) | [MPa] | 6.10 |
| Tensile strength $f_{ct,m}$ (mean) | [MPa] | 4.07 |
| Compression cube strength $f_{cc,m}$ (mean) | [MPa] | 43.60 |
| Compression cylindrical strength $f_{c,m}$ | [MPa] | 34.88 |
| Secant modulus of elasticity $E_{c,m}$ (mean) | [GPa] | 25.10 |
| **Steel reinforcement** – properties taken from [34] | | |
| Yield strength $f_y$ (nominal) | [MPa] | 500 |
| Modulus of elasticity $E_s$ (mean) | [GPa] | 200 |

The aim of loading tests was to verify the actual load-carrying capacity, deformation and deflection and real failure mechanism of test specimens, with regard both to the informative comparison of the different reinforcement types of developed panels, and to the verification of the accurate calculating model, but primarily, the loading tests should verify the possibility of the usage of these components in floor or roof structures, respectively, in comparison with usual traditional reinforced-concrete panels.

## III. Loading Test Performing

Test specimens have been simply supported on both opposite shorter sides with the bearing width of 50 mm in the support. Then, if the total length is 4 510 mm, the real span of the panel is $L$ = 4 460 mm. The typical shots of loading tests and their principle are illustrated in Fig. 3.

Fig. 3 Illustration of loading tests realized using vacuum loading test method

The photos of experiments illustrate the unique and effective method of the vacuum loading of plate components (author J. Melcher – see [5], [7] and Fig. 3), which has been developed, elaborated in detail and in the long term used in the test room of the authors' workplace. The effect of full uniform loading is caused using vacuum method when the supported slab specimen is installed to the timber testing box represented by rigid frame. The tested panel is together with the frame covered by transparent plastic matter foil glued to the floor. Air is sucked out of this closed space, that tested specimen is uniformly loaded overall on its area due to atmospheric overpressure.

The mode of the uniform loading or unloading can be simply regulated and loading intensity can be determined by measuring the overpressure between outside and inside space of the box.

During loading tests the slab components have been subjected by the uniform loading in the steps. The size of the interval of load increasing is chosen that the whole range of the load is divided to 10 steps minimally.

For the deflection measurement the digital and mechanical sensors with the accuracy of $10^{-2}$ have been used. The overpressure caused by the vacuum loading has been measured using the electric sensors with the digital indicator of the pressure and, for the control, in parallel it has been verified by the liquid manometer. During the loading process the "load- deflection" relationship has been monitored.

The loading has been applied up to the failure of test specimens. The primary outcomes of loading tests are the knowledge on the strain and failure mechanisms during the loading process and also in the moment of reaching the objective load-carrying capacity. To obtain the basic information about the influence of loading and unloading on the support bearing and permanent deformations, the loading effect was applied in the periodical repeated cycles.

## IV. Loading Test Results

The results of the measuring the "load – deflection" relationships during the loading process have been graphically elaborated by drawing the increase in deflections in the points 1 to 15 in the meaning of the scheme in Fig. 1.

The reaching load-carrying capacities are listed in Table 3 (all values taken from [1]). Appropriate photographs illustrate failures of the particular test specimens in the moment of reaching their objective ultimate load-carrying capacity.

Table 3 Load-carrying capacities (see [1])

| **Specimen** | **Full uniform load** | | |
|---|---|---|---|
| | self weight | maximum test load | **load-carrying capacity** |
| | $g$ [kNm$^{-2}$] | $p_{u,test}$ [kNm$^{-2}$] | $q_{u,test} = g + p_{u,test}$ [kNm$^{-2}$] |
| ***"A"*** ( ≡ 1) | 1.64 | 18.00 | **19.64** |
| *"B"* ( ≡ 2) | Not tested (see text above) | | |
| ***"C"*** ( ≡ 3) | 1.62 | 15.78 | **17.40** |
| ***"D"*** ( ≡ 2) | 1.54 | 5.79 | **7.33** |

### A. *Test Specimen "A"*

The overall arrangement of the test equipment prepared for the test specimen *"A"* is illustrated in Fig. 4, from which the test realization is evident, too.


Fig. 4 Illustration of loading test of specimen *"A"*

The load-carrying capacity $q_{u,test}$ of the specimen *"A"* given as the sum of the maximum load $p_{u,test}$ and self weight $g$ (see Table 3) is 19.64 kNm$^{-2}$ expressed as the uniform load, which corresponds to the value of 12.96 kNm$^{-1}$ per meter. Then, the corresponding bending moment is $M_{test}$ = 32.22 kNm.

The dependence of the deflection $w$ on the effect of the full uniform loading $p$ (excluding the self weight of the panel) for measured points (1 to 15) of the specimen *"A"* is shown from the graph in Fig. 5. It is evident that the slab of the floor panel supported on the longitudinal ribs has enough transverse stiffness and practically does not deflect on the line rectangular to the specimen span. The deflections in measured points on all transverse lines are practically the same.

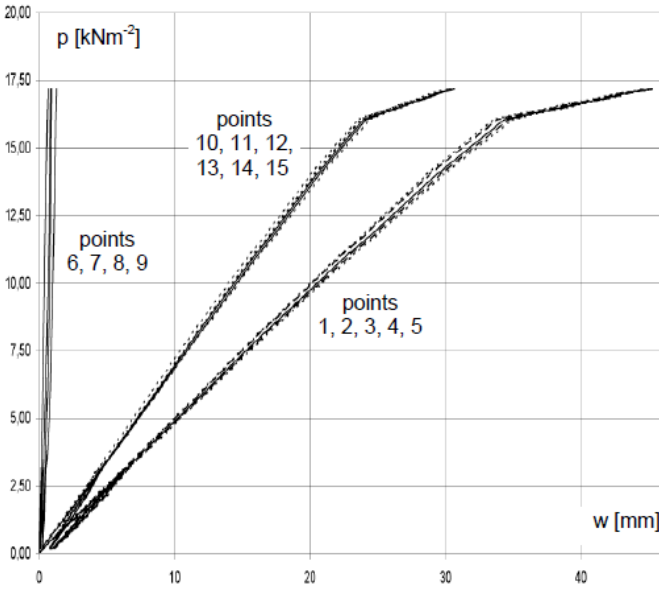


Fig. 5 Test specimen *"A"*: *"p – w"* relationship (see [1], [3])

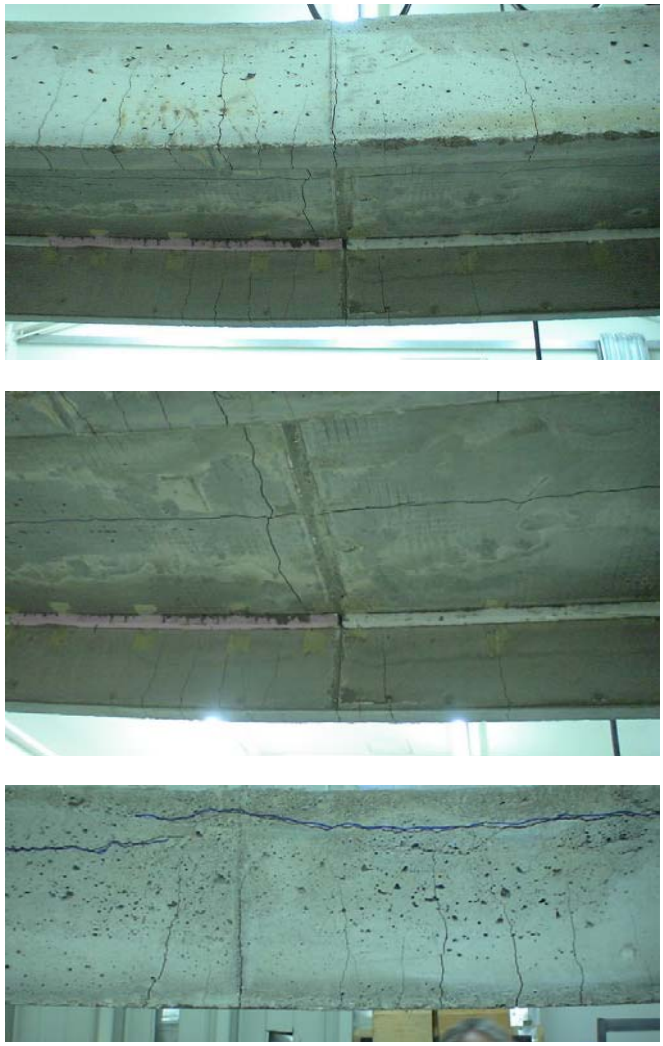

Fig. 6 Test specimen *"A"*: failure mechanism

The failure mechanism of the test specimen *"A"* is evident from Fig. 6. This figure shows the cracks on the edges of the longitudinal ribs and in the thin-walled slab in the middle-span zone. From these shots also the direction of the cracks initialized along the reinforcing bars are very good seen. In the view from bottom the location of the reinforcing wire mesh in the panel slab is visible. The reinforcing wire mesh ensures the integrity of the slab (unlike the test specimen *"C"* – see below, which is not provided with the mesh), so that the final failure of the specimen "A" occurred by reaching the yield strength in the main steel reinforcement.

### B. *Test Specimen "C"*

The illustration of the preparation and realization of the loading test of the specimen *"C"* is shown in Fig. 7.

The load-carrying capacity of the specimen *"C"* is given by the load $q_{u,test}$ = 17.40 kNm$^{-2}$ (see Table 3), i.e. 11.48 kNm$^{-1}$. The corresponding bending moment is $M_{test}$ = 28.54 kNm.

The relationships between the deflection $w$ and the loading effect $p$ (above the self weight of the panel) for the specimen *"C"* in measured points 1 to 15 are drawn in Fig. 8.

The specimen *"C"* has (among all components) the most effective main longitudinal reinforcement of the edge ribs and slab, which gives assumptions for comparably the best load-carrying capacity and stiffness of the specimen as a whole. However, reaching this load-carrying capacity is eliminated by the low, not-enough load-carrying capacity of the slab, which is not stiffened by the reinforcing wire mesh.


Fig. 7 Illustration of loading test of specimen *"C"*

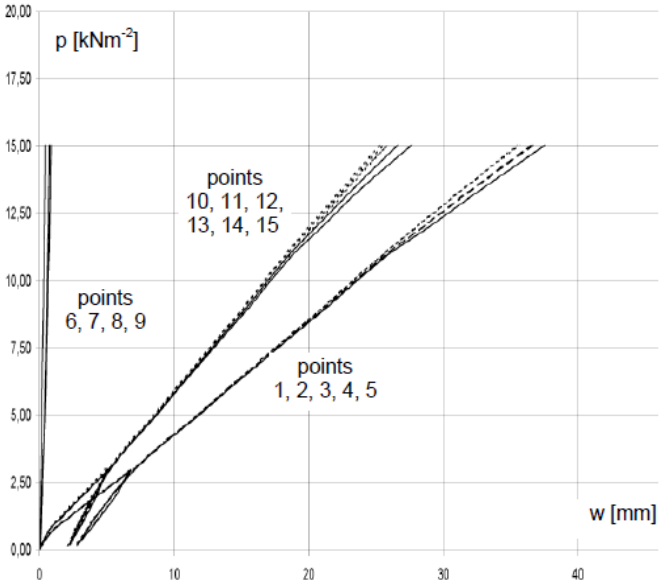


Fig. 8 Test specimen *"C"*: *"p – w"* relationship (see [1], [3])

Fig. 9 Test specimen *"C"*: failure mechanism

The failure mechanism of the test specimen *"C"* is evident from Fig. 9. In this case the slab of the tested specimen does not have enough load-carrying capacity because the slab has been failed by braking through practically on the whole length excluding support zones, where the positive influence of the end transverse rib was shown.

The absence of the reinforcing wire mesh causes the brittle fracture of the panel top slab. In Fig. 9 the lines of the failure along the lines of reinforcing bars are very good visible. The unreinforced slab is the weakest part of the panel, so that the slab failure occurs as a result of the reaching the compression strength of ferro-cement matrix before the reaching the yield strength of the main steel reinforcement (as occurred in the case of the specimen *"A"*).

### C. Test Specimen "D"

The illustration of the arrangement and realization of the loading test of the specimen *"D"* is shown in Fig. 10.

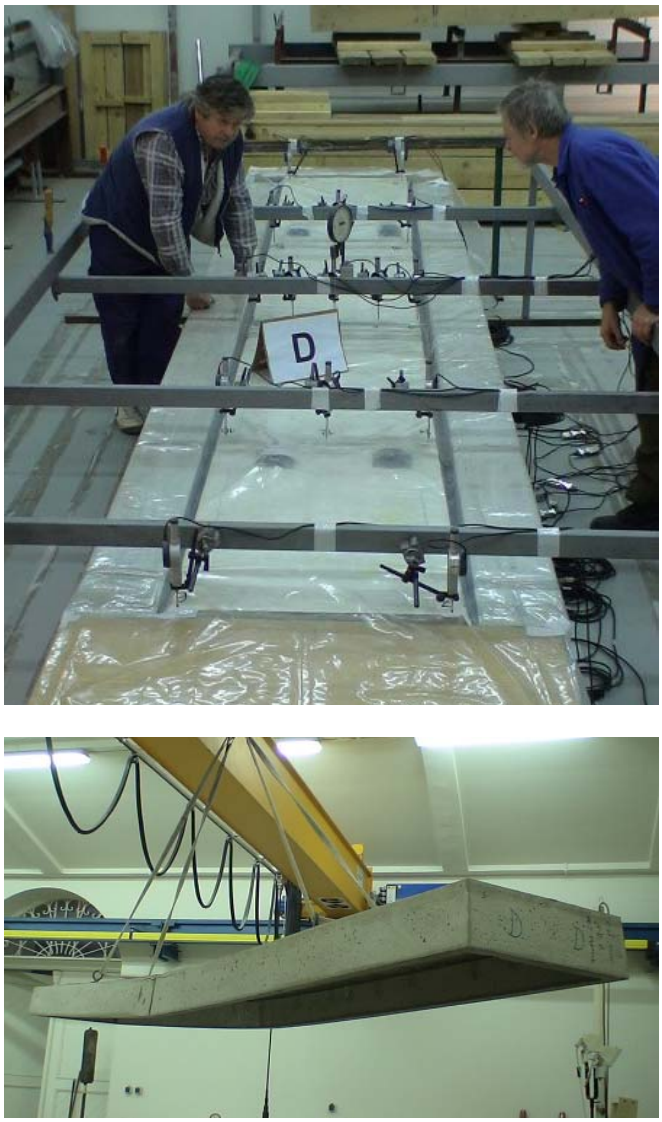


Fig. 10 Illustration of loading test of specimen *"D"*

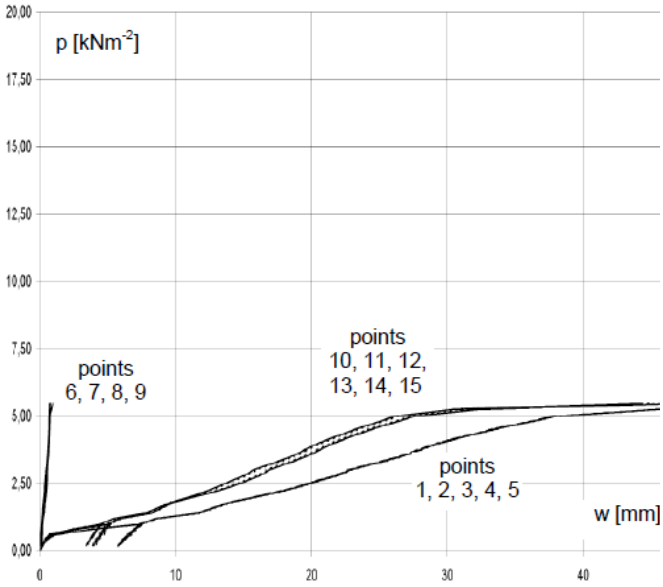


Fig. 11 Test specimen *"D"*: *"p – w"* relationship (see [1], [3])

The graph of the deflection $w$ due to the loading effect $p$ (above the self weight of the panel) in the measured points (1 to 15) of the specimen *"D"* is drawn in Fig. 11.

Fig. 12 Test specimen *"D"*: failure mechanism

The load-carrying capacity of the specimen *"D"* is given by the load $q_{u,test}$ = 7.33 kNm$^{-2}$ (see Table 3), i.e. 4.84 kNm$^{-1}$ (per

meter). The bending moment corresponding with the load-carrying capacity is $M_{test}$ = 12.03 kNm. The load-carrying capacity of the specimen *"D"* is less than a half of the load-carrying capacity of the specimens *"A"* and *"C"*. It is caused by the reinforcement, which is weaker than in other two cases, even if the assumed load-carrying capacity determined theoretically was noticeably higher than test one.

The failure mechanism of the specimen *"D"* is shown by the shots in Fig. 12. It is seen, that the load-carrying capacity of this panel is determined by the failure of longitudinal edge ribs and probably by reaching reinforcement yield strength.

It is evident, that the specimen *"D"* with comparably the smallest dimensions of the longitudinal reinforcement has significantly lower load-carrying capacity than has been verified in the case of specimens *"A"* and *"C"*. The ultimate load is minimal, that overload nor primer failure of the slab does not occur, although no reinforcing wire mesh is in the slab. The low stiffness of the slab is also evident from the relationship *"w – p"* on all transverse lines of the test specimen, which are practically the same.

## V. Test Results Evaluation and Conclusions

Based on the particular test results and their analysis the following conclusions and recommendations can be deducted for the investigated type of test specimens the initial overall conclusions:

- The experimental results document the load-carrying capacity of particular test specimens (see Table 3) and corresponding relationships "load $p$ – deflection $w$" (see Figs. 5, 8, 11) allowing to define the conventional load-carrying capacity according to the limit deflection.
- The load-carrying capacity following from the dimensions of the main longitudinal reinforcement of the ribs and slab requires the optimal transverse reinforcing of the slab, which cannot cause primary initiation of the failure of whole component.
- Experimentally verified objective load-carrying capacity of test specimens and corresponding "load $p$ – deflection $w$" relationships allow verifying calculating models.

### A. Failure Mechanisms and Load-Carrying Capacities

From the test results it is seen, the objective load-carrying capacities of all three specimens are different. Especially the load-carrying capacity of the specimen *"D"* is significantly lower in comparison with the load-carrying capacities of the specimen *"C"* with the same configuration and arrangement, but different dimensions of the main reinforcement. One of the aims of the loading tests was, inter alia, to investigate and evaluate the type of reinforcement from the viewpoint of its configuration and dimensions.

The low value of the objective load-carrying capacity of the specimen *"D"* is understandably given by the fact, that the cross-section area of the main reinforcement is significantly less, and that about only one-third (32.6 %) of the main reinforcement section area of the specimen *"C"*. However, the objective load-carrying capacity of the specimen *"D"* is surprisingly higher than expected, and that about 42 % of the load-carrying capacity of the specimen *"C"*. Even though, the load-carrying capacity of the specimen *"D"* is incomparable with load-carrying capacities of other specimens, that the arrangement of the specimen *"D"*, mainly with regards to the reinforcement dimensions, is not suitable and this type of the ferro-cement panel has not been further considered for the next practical application.

The objective load-carrying capacities of the specimens *"A"* and *"C"* are comparable, although the configuration of both specimens is different, especially from the viewpoint of the reinforcement arrangement and dimensions. The specimen *"A"* has the smaller dimensions of the main reinforcement than the specimen *"C"* (see Table 1), but it is compensated by the reinforcing wire mesh in the top slab of the panel. As it has been demonstrated by the test results, the influence of the reinforcing mesh has been proved very positive. Although the objective load-carrying capacities are not very different, the typical characters of the failure mechanism are fundamentally different. The reinforcing wire mesh can significantly increase the resistance and mainly toughness of the slab, that then in the case of the specimen *"A"* the slab failure does not occur (see Fig. 6), unlike the specimen *"C"*, where the slab failure occurs by the brittle fracture (see Fig. 9).

Based on the results mentioned above, ferro-cement panels of the configuration according to the specimen *"A"* have been considered for the subsequent investigation. Subsequently the next loading tests have been realized (not presented here) and the theoretical calculations have been performed for this type of ferro-cement panel (see [2]).

### B. Comparison of Test Results with Theoretical Calculations

Based on the usual calculating procedures taken from the available documents for the design of concrete structures the theoretical analysis of the investigated ferro-cement structural members has been performed with respect to the ultimate limit state and serviceability limit state too. The analysis was aimed to obtain the assumed resistances expected for the structural detailing and reinforcement dimensions corresponding with the configuration of the test specimen *"A"* and for the test specimens mechanical parameters, which have been measured using material testing in the case of ferro-cement matrix, or respectively, have been taken from the normative documents in the case of steel reinforcement (as mentioned above).

The resistance has been calculated in accordance with the progress of the failures during loading process and with the final failure mechanism occurred at the moment of reaching maximum load. The specimen *"A"*, for the results of which the analysis was performed, has been failed by the bending moment. When the tensile strength of the base material (ferro-cement matrix) has been reached, the first bending crack has been initialized, and subsequently, when the load has been increased, the significant crack propagation occurred. During loading process, the gradual raising of the specimen deflection and the continuous initialization of tensile cracks lengthwise

practically along the entire length of the specimen occurred. The test has been finished, when the yield strength of the reinforcement has been reached.

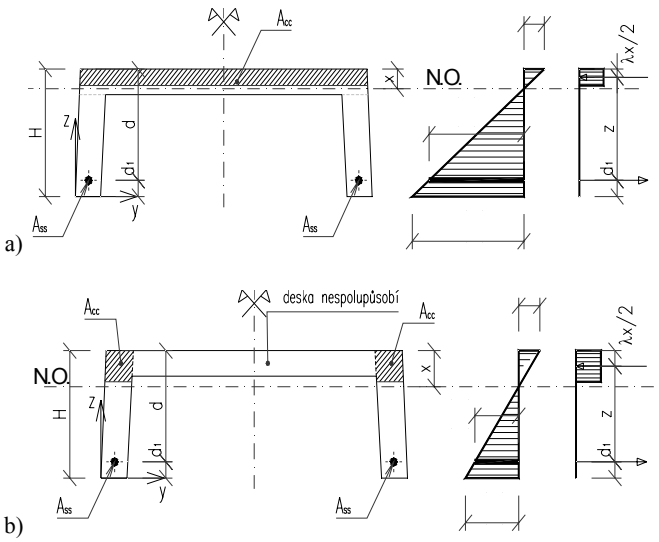


Fig. 13 Distribution of deformation and forces and stresses in the cross-section – plastic behaviour (taken from [2]):
a) interaction of slab with ribs (compression zone overall slab);
b) no interaction (compression zone in ribs only)

The bending moment resistances have been calculated assuming the reaching ultimate plastic capacity of one or more particular materials in the member section. The total load-carrying capacity is determined by the full utilization of ferro-cement matrix in compression and the bar reinforcement in tension. From the viewpoint of the interaction of the slab and ribs two alternative initial assumptions have been considered (see Fig. 13): a) the interaction of the slab and edge ribs was considered, so that the compression zone is assumed overall the cross-section top part, i.e. the top part of the slab and edge ribs, too; b) no interaction of the slab and ribs is considered, thus it is assumed the compression is transmitted by the edge ribs only, i.e. the compression zone is assumed in the top part of the ribs only.

The ultimate bending moment resistances $M_{Ru}$ have been calculated applying the general "method of the partial safety factors" given in [31]. For the calculation the following input parameters have been used: mean values of the mechanical properties of ferro-cement matrix (determined from material tests), nominal values of the mechanical properties of steel reinforcement (taken from [2], because the material tests have not been performed) and partial safety factors $\gamma_c$ (ferro-cement matrix) and $\gamma_s$ (reinforcement) by the values of $\gamma_c = \gamma_s = 1.0$. Thus, those theoretical capacities calculated can be considered practically as real maximum bending moments for the ultimate limit state. The values of ultimate bending moment capacities considering the assumptions above have been determined as:

in the case of a) $M_{Ru,a} = 25.60$ kNm (taken from [2]),

in the case of b) $M_{Ru,b} = 22.77$ kNm (taken from [2]).

Based on the comparison of theoretical moment resistances calculated above with the objective ultimate bending moment obtained from the loading test of the specimen *"A"* it can be noted, that the objective bending moment capacity obtained from the tests $M_{test} = 32.22$ kNm is: by 25.9 % higher than $M_{Ru,a} = 25.60$ kNm in the case of a); by 41.5 % higher than $M_{Ru,b} = 22.77$ kNm in the case of b). Taking into account that the design resistances used in the static assessment are usually much smaller than the calculated maximum resistances, and, of course, even much smaller than actual capacities obtained from the tests, it can be deducted, that the calculation utilized gives significant reserve and thus the sufficient safety. Then it can be concluded, that the theoretical approach, which has been utilized for the calculation of the bending moment capacity, can ensure the sufficient reliable structural design.

The test results have been indicatively compared with the theoretical analysis also from the viewpoint of serviceability limit state. For geometrical and mechanical parameters of the test specimens (see above) and for the maximum load reached at the moment of the total failure, the immediate deflection has been determined by the calculation, to compare it with the deflection obtained from the loading tests. The value of the immediate deflection in the middle-span of the beam has been calculated as $w = 32.9$ mm (taken from [2]). Based on the comparison with the test results it can be concluded, that the calculated deflection value approximately corresponds with the deflection obtained from the test of the specimen *"A"*.

In conclusion, it should be noted, that this research oriented to the development of ferro-cement structural components for the load-carrying structures of civil engineering constructions is currently continuing and it is aimed to the experimental verification of actual behaviour and failure mechanisms and theoretical analysis of load-carrying capacity not-only of the members with mentioned configuration, but also other types of structural components on the similar material base. The investigation is mainly focused on the effective utilization of the progressive structural materials represented by cement or concrete composites, usually composed of cement matrix and reinforcement made of materials of advanced properties, e.g. high-strength steel, carbon-fibre and glass-fibre reinforced polymers etc., but also composite components made of steel or timber combined with these high-performance materials. The development of all these materials and structural components composed of them aim to the efficient that means reliable and economy structural design. Some examples of the works and results of the research and development in this scientific field, which are related to the problem solved in this paper, are mentioned in the list of references (see e.g. [7] – [30]).

## ACKNOWLEDGEMENT

The paper has been elaborated within the framework of the research projects of the Czech Ministry of Education, Youth and Sports and the Czech Science Foundation: research centre project CZ.1.05/2.1.00/03.0097 ("AdMaS"), specific research project FAST S-11-32/1252, grant project No. 103/09/H085.

## REFERENCES


[1] J. Melcher et al., *Loading tests of ferro-cement components – 1st stage* (original in Czech language), Report for the company DAKO Brno, Ltd., Brno University of Technology, Faculty of Civil Engineering, Institute of Metal and Timber Structures, Brno, 2008, 18 pp.

[2] P. Štěpánek, B. Zmek and F. Girgle, *Solution of ferro-cement elements* (original in Czech language), Report for 2009 year – Stage 3a, b, Brno University of Technology, Faculty of Civil Engineering, Institute of Concrete and Masonry Structures, Brno, 2009, 30 pp.

[3] M. Karmazínová, J. Melcher and M. Štrba, "Loading tests of ferro-cement panels for horizontal slab structures", In *Proceedings of the 3rd European Conference on Civil Engineering "Recent Advances in Engineering"*, North Atlantic University Union, WSEAS Press: Paris, 2012, pp. 289-294. ISSN 2227-4588, ISBN 978-1-61804-137-1.

[4] J. Melcher, M. Karmazínová, M. Pilgr and M. Frank, *Defined load-carrying capacity of fibre-cements slabs – technology, tests, tables, graphs* (original in Czech language), VUSTAH Inc. & Faculty of Civil Engineering at Brno University of Technology: Brno, 2011, 102 pp.

[5] J. Melcher, "Full-scale testing of steel and timber structures: Examples and experience", In *Structural Assessment – The Role of Large and Full Scale Testing*, E&FN SPON: London, 1997, pp. 301-308. ISBN 0 419 22490 4.

[6] J. Melcher, "Design limit state: Reality or (science) fiction?", In *Proceedings of the International Conference on Advances in Steel Structures "ICASS'96"* held in Hong Kong, PERGAMON / Elsevier Science, Vol. I, 1996, pp. 579-584.

[7] J. Melcher, M. Karmazínová and M. Filip, "On design and experimental verification of actual behaviour of selected all-FRP structural components for civil engineering", In *Proceedings of the First Asia-Pacific Conference on FRP in Structures "APFIS 2007"*, University of Hong Kong, 2007, Vol. I, pp. 453-458. ISBN 978-962-8014-14-9.

[8] J. Melcher, M. Škaloud, M. Karmazínová and M. Zörnerová, "Experiment – A powerful tool applied in the solution of two important problems of the limit states of steel structures", In *Proceedings of the 1st International Conference on Advances in Experimental Structural Engineering "AESE 2005"* held in Nagoya, ICHIRYUSHA Publisher, Nagoya University / Aichi Institute of Technology: Nagoya, 2005, Vol. 1, pp. 83-92. ISBN 4-901887-18-1.

[9] M. Karmazínová, "Analysis of the actual behaviour, stress and moment capacity of composite beams composed of steel and glass-fibre-concrete", *International Journal of Mechanics*, Vol. 6, Issue 2, 2012, pp. 158-167. ISSN 1998-4448.

[10] M. Karmazínová, "Theoretical analysis and experimental verification of moment resistance of steel and timber beams strengthened by external CFRP composites", *International Journal of Mechanics*, Vol. 6, Issue 3, 2012, pp. 168-178. ISSN 1998-4448.

[11] M. Karmazínová, "Actual Behaviour of Composite Externally CFRP-Reinforced Timber Beams – Stress Analysis", *International Journal of Mechanics*, Vol. 7, Issue 1, 2013, pp. 1-9. ISSN 1998-4448.

[12] M. Karmazínová, "Design assisted by testing – a powerful tool for the evaluation of material properties and design resistances from test results", *International Journal of Mathematical Models and Methods in Applied Sciences*, Vol. 6, No. 2, 2012, pp. 376-385. ISSN 1998-0140.

[13] M. Karmazínová and J. J. Melcher, "Design assisted by testing applied to the determination of the design resistance of steel-concrete composite columns", In *Proceedings of the 13th WSEAS International Conference on Mathematical and Computational Methods in Science and Engineering*, WSEAS Press: Catania, 2011, pp. 420-425. ISBN 978-1-61804-046-6.

[14] J. Melcher, M. Karmazínová and M. Pilgr, "Evaluation of strength characteristics of fibre-cement slab material", *Advanced Materials Research,* Trans Tech Publication: 2013, Vol. 650, pp. 320-325. doi:10.4028/www.scientific.net/AMR.650.320.

[15] J. Melcher and M. Karmazínová, "Load-carrying capacity of cantilevers of anti-flood barriers made of FRP composite structural profiles", *Applied Mechanics and Materials*, Trans Tech Publications: 2013, Vols. 268-270, pp. 28-31. doi:10.4028/www.scientific.net/AMM.268-270.28.

[16] J. Melcher and M. Karmazínová, "Experimental verification and design of glass-FRP composite grids", In *Proceedings of the 2012 International Conference on Environmental and materials Engineering "EME 2012"* held in Seoul, *Advanced Materials Research,* Trans Tech Publications: 2012, 6 pp.

[17] Karmazínová, M., "Steel-concrete composite columns composed of high-strength materials – experimental analysis of buckling resistance", In *Proceedings of the 2012 2nd International Conference on Advances in Civil Engineering and Building Materials "CEBM 2012"*, CRC Press /Balkema, Hong Kong, 2012, pp. 755-760. ISBN 978-0-415-64342-9.

[18] J. J. Melcher and M. Karmazínová, "Influence of Atmospheric Physical Effects on Static Behavior of Building Plate Components Made of Fiber-Cement-Based Materials", In *Proceedings of the International Conference on Architectural and Civil Engineering "ICACE 2012"*, WASET: Bali 2012, Issue 0070, pp. 799-804. pISSN 2010-376X, eISSN 2010-3778.

[19] P. Bukovská, and M. Karmazínová, "Behaviour of the tubular columns filled by concrete subjected to buckling compression", *Procedia Engineering*, Vol. 40, 2012, pp. 68-73. doi:10.1016/j.proeng.2012.07.057.

[20] P. Bukovská, "Influence of Concrete Strength on the Behavior of Steel Tubular Columns Filled by Concrete", *International Journal of Mechanics*, Vol. 6, No. 3, 2012, pp. 149-157. ISSN 1998-4448.

[21] M. Karmazínová, M. Štrba and V. Kvočák, "Steel-concrete composite members using high-strength materials in building constructions – structural design, actual behaviour, application", In *Proceedings of the 2nd European Conference on Civil Engineering ("ECCIE'11")* "Recent Researchers in Engineering and Automatic Control", North Atlantic University Union, WSEAS: Puerto de la Cruz, 2011, pp. 47-52. ISBN 978-1-61804-057-2.

[22] Z. Kala, M. Karmazínová, J. Melcher, L. Puklický, A. Omishore, "Sensitivity analysis of steel-concrete structural members", In *Proceedings of the 9th International Conference on Steel-Concrete Composite and Hybrid Structures "ASCCS 2009"*, Research Publishing Services: Singapore, 2009, pp. 305-310. ISBN 978-981-08-3068-7.

[23] Z. Kala, L. Puklický, A. Omishore, M. Karmazínová and J. Melcher, "Stability problems of steel-concrete members composed of high-strength materials", *Journal of Civil Engineering and Management*, 2010, 16(3), pp. 352-362. doi: 10.3846/jcem.2010.40.

[24] M. Karmazínová, Actual stresses in CFRP-reinforced composite timber beams, In *Proceedings of the 7th WSEAS International Conference on Continuum Mechanics*, WSEAS Press: Kos Island, 2012, pp. 457-460. ISSN 2227-4359, ISBN 978-1-61804-110-4.

[25] J. Melcher, M. Karmazínová and J. Pozdíšek, "Experimental verification of behaviour of composite steel and glass-fibre-concrete beam", In *Proceedings of the 9th International Conference on "Steel-Concrete Composite and Hybrid Structures"* held in Leeds, Singapore: Research Publishing Services, 2009, pp. 390-395. ISBN 978-981-08-3068-7.

[26] J. Melcher and M. Karmazínová, "Strength characteristics of material of fiber-cement building components and verification of warming and sprinkling influence on their behavior" (original in Czech language), In *Proceedings of the XIVth International Conference on „Ecology and New Building Materials and Products"* held in Telč, pp. 291-294, VUSTAH Inc.: Brno, 2010. ISBN 978-80-87397-02- 2.

[27] J. Melcher, M. Karmazínová, J. Knězek and L. Lederer, "The influence of physical effects on behavior of structural components made of fiber-glass-concrete" (original in Czech language), In *Proceedings of the XIth Conference on „Ecology and New Building Materials and Products"* held in Telč, VUSTAH Inc.: Brno 2007, pp. 295-299. ISBN 978-80-239-9347-9.

[28] J. Melcher, M. Karmazínová, M. Knězek and L. Lederer, "Experimental verification of glass-fiber-concrete components of façade claddings" (original in Czech language), In *Proceedings of the Xth Conference on "Ecology and New Building Materials and Products"* held in Telč, VUSTAH Inc.: Brno, 2006, pp. 347-351. ISBN 80-239-7146-8.

[29] J. Melcher and M. Karmazínová, "Loading tests of glass-fiber-concrete façade panels stiffened by rib" (original in Czech language), In *Proceedings of the IXth Conference on "Ecology and New Building Materials and Products"* held in Telč, VUSTAH Inc.: Brno, 2005, pp. 204-208. ISBN 80-239-4905-5.

[30] J. Melcher, M. Karmazínová and J. Knězek, "Experimental verification of glass-fiber-concrete façade panels under wind loading actions" (original in Czech language), In *Proceedings of the VIth Conference on "New Building Materials and Products"* held in Telč, VUSTAH Inc.: Brno, 2002, pp. 52-55.

[31] ČSN EN 1992-1-1 (73 1201) *Eurocode 2: Design of Concrete Structures, Part 1-1: General Rules and Rules for Buildings*, the Czech Standard Institute, Prague, 2008.